Published in final edited form as:
Tetrahedron. 2008 September 1; 64(36): 8428–8434. doi:10.1016/j.tet.2008.05.047.

Pyrene-Appended Fluorescent Tweezers Generated via the Weak-Link Approach and Their Halide Recognition Properties

You-Moon Jeon, **Dongwoo Kim**, **Chad A. Mirkin***, **James A. Golen**†, and **Arnold L. Rheingold**†

Department of Chemistry and the International Institute for Nanotechnology, Northwestern University, 2145 Sheridan Road, Evanston, Illinois 60208-3113

†Department of Chemistry and Biochemistry, University of California, San Diego, 9500 Gilman Drive, MC 0358, La Jolla, California 92093-0358

Abstract

Through the Weak-Link Approach, fluorescent condensed and open Cu(I) tweezer complexes were prepared and characterized. These complexes exhibit fluorescence-sensitive binding properties for halide anions. The solid-state structure of a non-fluorescent Rh(I) tweezer analogue, determined by X-ray crystallography, shows that the counter anion, Cl^-, is trapped in between the two amide groups of the tweezer arms through hydrogen bonds. Although the tweezer binds Cl^-, the open complex also binds Cl^-, showing that the main role of the metal is to increase the local concentration of the pyrenyl amide moieties so that 2:1 binding can take place.

1. Introduction

Over the past decade, supramolecular cyclophanes and tweezer complexes have received a significant amount of attention due to their encapsulating properties and potential applications in catalysis, sensing, mixture separations, molecular electronics, and facilitated small molecule transport.[1–4] Our group has shown that one can prepare fluorescent cyclophanes[5] via the Weak-Link Approach (WLA) in high-yield (Scheme 1).[2,6] The strategically positioned weak ligand-metal interactions within these structures allow one to use small molecules and elemental anions to reversibly open and close such structures, allowing one to chemically trigger significant changes in their recognition and catalytic properties.[2]

Herein, we demonstrate how the WLA can be used to prepare a novel class of fluorescent tweezer complexes that incorporate both recognition sites and fluorophores within the framework of the ligand that makes up the tweezer arms. We compare the halide binding properties of these novel structures with the open versions of these structures.

*Corresponding author. Tel.: +1-847-491-2907; fax: +1-847-495-5123; chadnano@northwestern.edu.

Supplementary data

Supplementary data associated with this article can be found in the online version, at doi:xxxxx and the crystallographic data for **2** (CCDC 675487) and **3a** (CCDC 675488) can be obtained free of charge from the Cambridge Crystallographic Data Centre via www.ccdc.cam.ac.uk/data_request/cif.

2. Results and discussion

The pyrenyl group has been used as a signaling fluorophore, since when it dimerizes in the presence of analytes, it forms a characteristic excimer.[7] We hypothesized that two equivalents of such a moiety, held together in a tweezer configuration in the context of a coordination complex prepared via the WLA, could act as a characteristic signaling fluorophore for analyte recognition. The new pyrene-appended hemilabile phosphine ligand **2** was synthesized in two steps (Scheme 2) and fully characterized by ^{1}H, $^{31}P\{^{1}H\}$ NMR spectroscopy and mass spectrometry. The solid-state structure of **2** was confirmed via a single crystal X-ray diffraction study (Figure 1).

The Rh(I) tweezer complex **3a** was synthesized by the reaction of $[Rh(NBD)Cl]_2$ (NBD = norbornadiene) and hemilabile ligand **2** in CH_2Cl_2 at room temperature in quantitative yield (Scheme 3). It is insoluble in CH_2Cl_2 and forms as a yellow precipitate in the bottom of the reaction vessel. All data, including ^{1}H NMR spectroscopy in a 3:1 mixture of CD_2Cl_2 and CD_3OD, $^{31}P\{^{1}H\}$ NMR spectroscopy in the same solvent mixture, and ESI-MS, are in full agreement with the proposed structural formulation for **3a**. For example, the $^{31}P\{^{1}H\}$ NMR spectrum of **3a** exhibits a doublet at δ 64.7 ($J_{Rh\text{-}P}$ = 161 Hz) assigned to the equivalent phosphorous atoms. This chemical shift and coupling constant are highly diagnostic of a square planar *cis*-phosphine, *cis*-thioether Rh(I) complex.[2,8,9] Significantly, the amide hydrogen atoms are shifted downfield from where they would normally appear (*vide infra*). This is likely due to an interaction between those protons and the Cl^- counter ion. The ESI-MS spectrum of **3a** exhibited a peak at *m/z* 1261.5 corresponding to the loss of the Cl^- counter anion (Calcd. for $[M\text{-}Cl^-]^+$ = 1261.3).

The solid-state structure of **3a** (Figure 2), as determined by X-ray crystallography, is consistent with its proposed solution structure. The Rh(I) metal center is coordinated by two phosphines and two thioethers in a distorted square-planar geometry with P(1)-Rh(1)-S(1) and P(1)-Rh(1)-P(1′) angles of 85.21° and 98.46°, respectively. Each coordinating sulfur atom has a distorted trigonal pyramidal geometry with C(14)-S(1)-Rh(1), C(14)-S(1)-C(15), and C(15)-S(1)-Rh(1) angles of 105.7°, 102.0°, and 111.5°, respectively. Of particular interest is the chloride anion, which is trapped between the two amide groups through hydrogen bonds.[10] The N(1)…Cl(1) distance and the N(1)-H(1A)-Cl(1) angle are 3.24 Å and 162.4°, respectively. The two bridging aromatic spacers have a twisted configuration with a torsion angle of 74.5° owing to the trigonal pyramidal configuration of the coordinating sulfur atom and the coordination of the Cl^- anion. Note the pyrenyl groups in **3a** exhibit intermolecular π-π stacking interactions in the solid-state (the inter-plane distance of the two pyrenyl group is 3.7 Å, Figure S1).[11]

Upon reaction with CO (1 atm), the tweezer complex **3a** opens to form a neutral Rh(I) complex **4a** (CD_2Cl_2/CD_3OD = 3/1, Scheme 3).[2,4,9] This reaction involves the displacement of the thioether ligands of **3a** with one equivalent of CO and the Cl^- counter ion. The $^{31}P\{^{1}H\}$ NMR spectrum of **4a** exhibits a resonance at δ 25.0 (d, $J_{Rh\text{-}P}$ = 124 Hz) indicative of a complex with *trans*-coordination of the two phosphorous atoms.[2,4,9] Although complex **4a** is stable under CO (1 atm) at room temperature, exposure to high vacuum results in its conversion to the cationic condensed Rh(I) tweezer **3a**. The interconversion between complex **4a** and **3a** is completely reversible as evidenced by ^{1}H and $^{31}P\{^{1}H\}$ NMR spectroscopy. Note, the amide protons, which exhibit a resonance at δ 8.77 in **3a**, appear at δ 8.39 in **4a** in a 3:1 mixture of CD_2Cl_2 and CD_3OD (Figure S2).

In an attempt to increase the solubility of the condensed Rh(I) tweezer **3a**, the anion was changed from Cl^- to BF_4^- (**3b**) and $B(C_6F_5)_4^-$ (**3c**), respectively (Scheme 3). These complexes were prepared by initially abstracting the Cl^- from the Rh(I) precursor with the

appropriate reagent ($AgBF_4$ and $LiB(C_6F_5)_4$, respectively). The chemical shifts and coupling constants for the phosphorus atoms of **3b** and **3c** were nearly identical to those observed for **3a** (**3b**: δ 64.8 (d, $J_{Rh\text{-}P}$ = 161 Hz), **3c**: δ 64.7 (d, $J_{Rh\text{-}P}$ = 162 Hz)). Although **3a** and **3b** are not soluble in pure dichloromethane, **3c** with $B(C_6F_5)_4^-$ as the counter anion is highly soluble at room temperature. The ability of **3c** to bind Cl^- was studied by ^1H NMR titration experiments in CD_2Cl_2 solution at room temperature. In all experiments, the chemical shift for the amide −N*H* resonance was monitored as a function of Cl^- concentration. As expected, the amide proton signals shift downfield, indicative of strong interactions with the Cl^- (Figure 3b). The K_a of **3c** for Cl^- is 2.48×10^3 M^{-2} as determined by EQNMR techniques.[12] The interaction between Cl^- and **3c** is primarily with the tweezer arms. Indeed, there is no evidence of Cl^- interacting with the metal center as probed by $^{31}P\{^1H\}$ NMR spectroscopy. The doublet at δ 64 does not change significantly even in the presence of excess Cl^- without CO (Figure 3a). Interestingly, in the solution state, **3c** forms a 2:1 rather than a 1:1 complex with Cl^- as determined by a Job plot (Figure 4). Similar differences in stoichiometry, depending upon the physical state, have been observed with a bicycliccyclophane complex with Cl^- anion (1:1 in the solution state and 1:2 in the solid state).[13]

Since Rh(I) quenches the fluorescence associated with the pyrene based ligand, we turned to Cu(I) as an alternative metal hinge. Complex **3d**, the Cu(I) analogue of the Cl^- free Rh(I) tweezer complexes **3b** and **3c**, can be synthesized by the reaction of $[Cu(CH_3CN)_4][PF_6]$ and ligand **2** in CH_2Cl_2 at room temperature (Scheme 4). This methodology is similar to that used for preparing Cu(I) metallocyclophanes using the symmetrical 1,4-bis[2-(diphenylphosphino)ethylthio]benzene ligands.[14] All of the spectroscopic data, including ^1H NMR spectroscopy, $^{31}P\{^1H\}$ NMR spectroscopy, and ESI-MS are in full agreement with the proposed formulation for **3d**. For example, the $^{31}P\{^1H\}$ NMR spectrum of **3d** exhibits a broad singlet at δ 0.15 due to the interaction of the phosphorus atoms with the quadrupolar ^{63}Cu and ^{65}Cu nuclei (*I* =3/2), indicative of equivalent phosphorus atoms in the condensed Cu(I) tweezer complex.[3,14,15] Pyridine was chosen as a suitable N-donor for opening the Cu(I) condensed intermediates since it works quite well in the metallocyclophane cases.[3,14,15] Successful displacement of the Cu-S bonds in **3d** was achieved via the addition of excess pyridine, which results in the quantitative formation of the colorless cationic open Cu(I) tweezer **4d** (Scheme 4). The open Cu(I) tweezer **4d** was characterized by ^1H and $^{31}P\{^1H\}$NMR spectroscopy, ESI-MS, and elemental analysis. The complex exhibits a diagnostic resonance in its $^{31}P\{^1H\}$ NMR spectrum at δ −3.52, which is similar to what is observed for mono and binuclear open Cu(I) complexes with two phosphines and two pyridines (shift from δ − 0.05 to − 4.60).[3,14–16] Although complex **4d** is stable in CH_2Cl_2 solution as well as in solid state, under high vacuum, its ESI-MS spectrum exhibited only a single peak at *m/z* 1221.6 corresponding to the loss of two pyridine ligands and the PF_6^- counter anion (Calcd. for $[M - 2 \text{ pyridine} - PF_6^-]^+$ = 1221.3).

We investigated the absorption and emission properties of ligand **2**, condensed Cu(I) tweezer **3d**, and open Cu(I) tweezer **4d**. The Cu(I) complexes **3d** and **4d** in CH_2Cl_2 (with 5% DMF) and ligand **2** show nearly identical absorption spectra with λ_{max} at 345 nm. Emission spectra of **2**, **3d**, and **4d** with excitation at 345 nm in the same solvent system are different (Figure 5a). The metal complexes both exhibit broad and strong excimer bands at 475 nm, while the ligand does not. Interestingly, the relative intensity of excimer to monomer emission (I_E/I_M) is slightly larger in the open complex **4d** (I_E/I_M = 1.46) as compared with the condensed structure **3d** (I_E/I_M = 1.01). Presumably, the open structure provides the structural flexibility for the two pyrene moieties to interact more strongly than in the condensed structure. Open Cu(I) tweezer **4d** interacts with Cl^- as evidenced by an increase in fluorescence intensity of the excimer as a function of added chloride anion up to 1 equivalent (Figure 5b). The data are consistent with the formation of a structure analogous

to crystallographically characterized **3a** where the Cl^- enhances the interaction between the pyrene moieties via the halide induced chelation effect of the pyrene-appended two amide groups. If the titration is continued, the excimer intensity steadily decreases after one equivalent until it disappears at 100 equivalents. Note, the first Cl^- can be trapped inbetween the two amide groups but the additional anions tend to break the chelate conformation to make individual hydrogen bonding complexes for each amide group, which prohibits excimer formation. Condensed Cu(I) tweezer **3d** shows a similar recognition trend to that of **4d**, showing that although the metal site is important for holding two equivalents of ligand within one complex, the orientation of the pyrenes in the tweezer **3d** does not offer a significant advantage with respect to Cl^- recognition. Note that consistent with this conclusion the free base ligand **2** does not show any excimer formation in the presence of Cl^-(Figure S3a). The condensed and open tweezers **3d** and **4d** exhibit similar recognition trends with Br^- and I^- (Figure S3–S4).

3. Conclusions

We have developed a method for rapidly assembling fluorescent tweezer complexes from Cu(I) metal ion and the appropriate pyrene-appended hemilabile ligands. These complexes exhibit fluorescence-dependent binding properties for halide anions. X-ray crystallography of a non-fluorescent Rh(I) analogue shows that the Cl^- ion interacts with the amide moieties flanking the pyrenyl groups. Surprisingly, the pocket created by the condensed tweezer **3d** does not confer significant advantages with respect to halide binding or selectivity since the open structure **4d** shows very similar trend. Indeed, the main role of the metal is to increase the local concentration of the pyrenyl amide moieties so that 2:1 binding can take place.

4. Experimental

4.1. General

All reactions were carried out under an inert atmosphere of nitrogen using standard Schlenk techniques or an inert atmosphere glove box unless otherwise noted.[17] Diethyl ether, CH_2Cl_2, pentane, and hexanes were purified by published methods.[18] All solvents were deoxygenated with nitrogen prior to use. 2-Chloroethyldiphenylphosphine was purchased from Organometallics Inc. and used as is. Deuterated solvents were purchased from Cambridge Isotope Laboratories Inc. and used as received. $[Rh(NBD)Cl]_2$ (NBD is norbonadiene) was purchased from Stem Chemical Inc. and used as is. All other chemicals were used as received from Aldrich. ^1H NMR spectra were recorded on a Varian Mercury 300 MHz FT-NMR spectrometer and referenced relative to the residual proton resonances. $^{31}P\{^1H\}$ NMR spectra were recorded on a Varian Mercury 300 MHz FT-NMR spectrometer at 121.4 MHz and referenced relative to an external 85% H_3PO_4 standard. $^{19}F\{^1H\}$ NMR spectra were recorded on a Varian Mercury 300 MHz FT-NMR spectrometer at 282.47 MHz and referenced relative to an external $CFCl_3$ in $CDCl_3$ standard. All chemical shifts are reported in ppm. Electrospray ionization mass spectra (ESI-MS) were recorded on a Micromas Quatro II triple quadrapole mass spectrometer. Electron ionization mass spectra (EIMS) were recorded on a Fisions VG 70–250 SE mass spectrometer. Fluorescent spectra were recorded with a Hewlett Packard (HP) 8452a diode array spectrometer. Elemental analyses were performed by Quantitative Technologies Inc. Whitehouse, NJ.

4.2. Materials

4.2.1. $Ph_2PCH_2CH_2SC_6H_4CO_2H$ (1)—A mixture of 4-mercaptobenzoic acid (2.0 g, 12.32 mmol), 2-chloroethyldiphenylposphine (3.3 g, 13.14 mmol), potassium carbonate (6.0 g, 42.98 mmol), and 18-crown-6 (0.5 g, 1.89 mmol) in acetonitrile/H_2O (80/20 mL) was

heated at reflux with vigorous stirring over night. The mixture was allowed to cool to room temperature and conc. HCl was added dropwise to make the solution acidic under ice bath cooling. The precipitate was filtered and washed with water, CH_2Cl_2, acetone, and diethyl ether successively and dried *in vacuo*, which gave analytically pure white solid (3.7 g, 82 %). ^{1}H NMR (DMF-d_7): δ 2.66 (m, 2H, - CH_2PPh$_2$), 3.32 (m, 2H, J = 7.2 Hz, -CH_2S-), 7.46–7.69 (m, 12H, -C$_6H_4$-, -P(C$_6H_5$)$_2$), 8.07 (d, 2H, -C$_6H_4$-). ^{31}P{^{1}H} NMR (DMF-d$_7$): δ −16.32 (s). MS (EI, m/z) = 366.1 (Calcd. for $C_{21}H_{19}O_2PS$ = 366.0). Elemental analysis for $C_{21}H_{19}O_2PS{\cdot}C_4H_{10}O$ Calcd.: 68.16% C, 6.64% H. Found: 68.29% C, 6.95% H.

4.2.2. Ph$_2$PCH$_2$CH$_2$SC$_6$H$_4$CONHCH$_2$(C$_{16}$H$_9$) (2)—Chloro *i*-butylformate (0.1 mL, 0.72 mmol) was added dropwise to the CH_2Cl_2 (10 mL) solution of **1** (0.2 g, 0.55 mmol) and triethylamine (0.1 mL, 0.72 mmol) under ice-bath cooling for 5 min and stirred 1 h at room temperature. To the solution 2-pyrenylmethylamine·HCl (0.17 g, 0.60 mmol) and triethylamine (3 mL, 21.52 mmol) in CH_2Cl_2 (10 mL) were added dropwise and stirred for 2 h at room temperature. Solvent was evaporated at reduced pressure and the remaining solid was washed with acidic ethanol. The desired product was isolated by filtration and dried under vacuum (70 mg, 22%). ^{1}H NMR (THF-d_8): δ 2.36 (m, 2H, -CH_2PPh$_2$), 2.99 (m, 2H, -CH_2S-), 5.31 (d, 2H, J = 5.7 Hz, -CH_2N-), 7.17 (d, 2H, J = 6.6 Hz, -C$_6H_4$-), 7.19–7.42 (m, 10H, -P(C$_6H_5$)$_2$), 7.77 (d, 2H, J = 6.6 Hz, -C$_6H_4$-), 7.96–8.20 (m, 8H, Pyrene-*H*), 8.47 (d, 1H, J = 9.0 Hz, Pyrene-*H*). ^{31}P{^{1}H} NMR (THF-d_8): δ −15.92 (s). HRMS (EI, m/z) = 579.1790 (Calcd. for $C_{38}H_{30}NOPS$ = 579.1786). Elemental analysis for $C_{38}H_{30}NOPS{\cdot}1/2CH_2Cl_2$ Calcd.: 74.32% C, 5.02% H, 2.25% N. Found: 74.40% C, 5.58% H, 1.82% N.

4.2.3. [(Ph$_2$PCH$_2$CH$_2$SC$_6$H$_4$CONHCH$_2$(C$_{16}$H$_9$))$_2$Rh][Cl] (3a)—The dichloromethane solution (20 mL) of ligand **2** (200 mg, 345.0 μmol) and [Rh(NBD)Cl]$_2$ (40 mg, 85.9 μmol) was stirred overnight at room temperature. Solvent was evaporated under reduced pressure. The resulting yellow precipitate was washed with THF and diethyl ether and dried *in vacuo* (215 mg, 96%). ^{1}H NMR (CD_2Cl_2/CD_3OD=3/1): δ 2.51 (m, 4H, -CH_2PPh$_2$), 2.70 (m, 4H, -CH_2S-), 5.06 (d, 4H, J = 5.5 Hz, -CH_2N-), 7.19–7.34 (m, 24H, -C$_6H_4$-, -P(C$_6H_5$)$_2$), 7.51 (d, 4H, J = 6.6 Hz, -C$_6H_4$-), 7.88–8.06 (m, 16H, Pyrene-*H*), 8.15 (d, 2H, Pyrene-*H*), 8.77 (br t, 2H, J = 9.3 Hz, -N*H*-). ^{31}P{^{1}H} NMR (CD_2Cl_2/CD_3OD=3/1): δ 64.70 (d, $J_{Rh\text{-}P}$ = 161 Hz). MS (ESI, m/z): [M - Cl]$^+$ = 1261.5 (Calcd. for $[C_{76}H_{60}N_2O_2P_2RhS_2]^+$ = 1261.2). Elemental analysis for $C_{76}H_{64}N_2O_2P_2RhS_2Cl{\cdot}1/2CH_2Cl_2$ Calcd.: 68.56% C, 4.59% H, 2.09% N. Found: 68.37% C, 4.22% H, 2.11% N.

4.2.4. [(Ph$_2$PCH$_2$CH$_2$SC$_6$H$_4$CONHCH$_2$(C$_{16}$H$_9$))$_2$Rh] [BF$_4$] (3b)—The dichloromethane solution of [Rh(NBD)Cl]$_2$ (40 mg, 85.9 μmol) and $AgBF_4$ (35 mg, 179.8 μmol) was stirred for 10 min at room temperature. The solution of Rh(I) precursor in dichloromethane was added to dichloromethane solution of ligand **2** (200 mg, 345.0 μmol) dropwise and stirred overnight at room temperature. Solvent was evaporated under reduced pressure and the resulting yellow precipitate was washed with THF and dried *in vacuo* (189 mg, 81%). ^{1}H NMR (CD_2Cl_2/CD_3OD=3/1): δ 2.56 (m, 4H, -CH_2PPh$_2$), 2.78 (m, 4H, -CH_2S-), 5.08 (s, 4H, -CH_2N-), 7.25–7.56 (m, 28H, -C$_6H_4$-, -P(C$_6H_5$)$_2$), 7.74–8.22 (m, 18H, Pyrene-*H*). ^{31}P{^{1}H} NMR (CD_2Cl_2/CD_3OD=3/1): δ 64.78 (d, $J_{Rh\text{-}P}$ = 161 Hz). MS (ESI, m/z): [M - BF_4^-]$^+$ = 1261.6 (Calcd. for $[C_{76}H_{60}N_2O_2P_2RhS_2]^+$ = 1261.2). Elemental analysis for $C_{76}H_{60}BF_4N_2O_2P_2RhS_2{\cdot}2CH_2Cl_2$ Calcd.: 61.68% C, 4.25% H, 1.84% N. Found: 61.90% C, 4.21% H, 1.74% N.

4.2.5. [(Ph$_2$PCH$_2$CH$_2$SC$_6$H$_4$CONHCH$_2$(C$_{16}$H$_9$))$_2$Rh] [B(C$_6$F$_5$)$_4$] (3c)—The desired complex **3c** was synthesized by similar method to that of **3b** using [Rh(COD)Cl]$_2$ (40 mg, 79.5 μmol), LiB(C$_6$F$_5$)$_4$·Et$_2$O (130.0 mg, 171.0 μmol), and ligand **2** (185 mg, 319.1 μmol).

The product was washed with diethyl ether and dried under vacuum (229 mg, 74%). ^{1}H NMR (CD_2Cl_2): δ 2.49 (m, 4H, -CH_2PPh$_2$), 2.66 (m, 4H, -CH_2S-), 5.07 (d, 4H, J = 5.7 Hz, -CH_2N-), 7.20–7.45 (m, 28H, -C$_6H_4$-, -P(C$_6H_5$)$_2$), 7.88–8.15 (m, 18H, Pyrene-*H*). ^{31}P{^{1}H} NMR (CD_2Cl_2): δ 64.67 (d, J_{Rh-P} = 162 Hz). ^{19}F NMR (CD_2Cl_2): δ −133.49 (s), −146.03 (t), −167.90 (d). MS (ESI, m/z): [M - B(C$_6F_5$)$_4$]$^+$ = 1261.5 (Calcd. for [$C_{76}H_{60}N_2O_2P_2RhS_2$]$^+$ = 1261.2). Elemental analysis for $C_{101}H_{62}BCl_2F_{20}N_2O_2P_2RhS_2$·$CH_2Cl_2$ Calcd.: 59.87% C, 3.08% H, 1.38% N. Found: 59.90% C, 2.72% H, 1.28% N.

4.2.6. [(Ph$_2$PCH$_2$CH$_2$SC$_6$H$_4$CONHCH$_2$(C$_{16}$H$_9$))$_2$Cu] [PF$_6$] (3d)—To the suspension of ligand **2** (91 mg, 0.157 mmol) in dichloromethane (10 mL), dichloromethane solution of [(CH$_3$CN)$_4$Cu]PF$_6$ (30 mg, 0.079 mmol) was added dropwise and stirred overnight at room temperature. Solvent was evaporated under reduced pressure and dried *in vacuo* overnight. Diethyl ether was added and sonicated for 10 min. White precipitate was isolated by filtration and dried under vacuum (103 mg, 96%). ^{1}H NMR (CD_2Cl_2): δ 2.69 (br s, 4H, -CH_2PPh$_2$), 3.21 (br s, 4H, -CH_2S-), 5.21 (br s, 4H, -CH_2N-), 6.80 (br s, 2H, -N*H*-), 7.09 (d, 4H, J = 6.6 Hz, -C$_6H_4$-), 7.32–7.45 (m, 20H, -P(C$_6H_5$)$_2$), 7.75 (d, 4H, J = 6.9 Hz, -C$_6H_4$-), 7.95–8.17 (m, 16H, Pyrene-*H*), 8.31 (d, 2H, J = 9.0 Hz, Pyrene-*H*). ^{31}P{^{1}H} NMR (CD_2Cl_2): δ 0.15 (br s, -PPh$_2$), −143.20 (m, PF$_6^-$). MS (ESI, m/z): [M - PF$_6^-$]$^+$ = 1221.4 (Calcd. for [$C_{76}H_{60}N_2O_2P_2CuS_2$]$^+$ = 1221.3). Elemental analysis for $C_{76}H_{60}CuF_6N_2O_2P_3S_2$·1.5$CH_2Cl_2$ Calcd.: 62.25% C, 4.25% H, 1.87% N. Found: 62.25% C, 3.84% H, 1.52% N.

4.2.7. [(Ph$_2$PCH$_2$CH$_2$SC$_6$H$_4$CONHCH$_2$(C$_{16}$H$_9$))$_2$Rh(CO) Cl] (4a)—To the solution of complex **3a** in a 3:1 mixture of CD_2Cl_2 and CD_3OD was charged with CO gas (1 atm) for 10 min, which gave a desired open complex in quantitative yield. ^{1}H NMR (CD_2Cl_2/CD_3OD=3/1): δ 2.68 (br m, 4H, - CH_2PPh$_2$), 2.90 (br m, 4H, -CH_2S-), 5.20 (d, 4H, J = 5.4 Hz, -CH_2N-), 7.10 (d, 4H, J = 7.5 Hz, -C$_6H_4$-), 7.36–8.15 (m, 40H, -C$_6H_4$-, -P(C$_6H_5$)$_2$, -Pyrenyl-*H*), 8.28 (d, 2H, J = 9.0 Hz, -Pyrenyl-*H*), 8.39 (br t, 2H, -N*H*-). ^{31}P{^{1}H} NMR (CD_2Cl_2/CD_3OD=3/1): δ 25.06 (d, J_{Rh-P} = 124 Hz). Alternatively, the complex **4a** can be synthesized from **3b** and **3c** by the reaction of 1 equiv of *n*-Bu$_4$N$^+$Cl$^-$ and CO gas (1 atm) in CH_2Cl_2 at room temperature in quantitative yield.

4.2.8. [(Ph$_2$PCH$_2$CH$_2$SC$_6$H$_4$CONHCH$_2$(C$_{16}$H$_9$))$_2$Cu (Pyridine)$_2$][PF$_6$] (4d)—Excess amount of pyridine (1 mL) was added to the solution of **3d** (95 mg, 69.0 μmol) in dichloromethane (10 mL) and stirred for 30 min at room temperature. Solvent was evaporated under reduced pressure and dried *in vacuo* overnight. Diethyl ether was added and sonicated for 10 min. White precipitate was isolated by filtration and dried under vacuum (97 mg, 92%). ^{1}H NMR (CD_2Cl_2): δ 2.52 (br s, 4H, -CH_2PPh$_2$), 3.00 (br s, 4H, -CH_2S-), 5.14 (br d, 4H, J = 4.8 Hz, -CH_2N-), 6.74 (br d, 4H, J = 5.4 Hz, -C$_6H_4$-), 7.30–7.50 (m, 28H, -P(C$_6H_5$)$_2$, Pyridine, Pyrene-*H*), 7.73 (t, 2H, J = 7.8 Hz, Pyrene-*H*), 7.91–8.24 (m, 18H, Pyridine, Pyrene-H), 8.42 (br s, 4H, Pyridine). ^{31}P{^{1}H} NMR (CD_2Cl_2): δ −3.52 (br s, -*P*Ph$_2$), −143.22 (m, *P*F$_6^-$). MS (ESI, m/z): [M - 2Pyridine - PF$_6^-$]$^+$ = 1221.6 (Calcd. for [$C_{76}H_{60}N_2O_2P_2CuS_2$]$^+$ = 1221.3). Elemental analysis for $C_{86}H_{70}CuF_6N_4O_2P_3S_2$ Calcd.: 67.68% C, 4.62% H, 3.67% N. Found: 67.35% C, 4.50% H, 3.53% N.

4.3. X-ray crystallography

4.3.1. Refinement—Crystals **2** and **3a** were mounted on a CryoLoop© with Paratone-N© oil and immediately placed under a liquid stream of N_2 on a Bruker SMART APEX CCD system respectively. Data collected at −60 °C with Mo Kα radiation and corrected for absorption using the SADABS program. Structure was solved by Patterson difference map, developed by successive difference Fourier syntheses, and refined by full matrix least

squares on all F^2 data. All non-hydrogen atoms were refined as being anisotropic and hydrogen atoms except H1A on N1 in **3a** were placed in calculated positions with temperature factors fixed at 1.2 or 1.5 times the equivalent isotropic U of the C atoms to which they were bonded. Hydrogen atom H1A was determined from a Fourier difference map and allowed to refine.

4.3.2. Crystallographic data—For **2** (CCDC 675487): $C_{38}H_{30}NOPS$, monoclinic, space group *P*2(1)/c, *a* = 16.115(2) Å, *b* = 9.778(1) Å, *c* = 18.536(2) Å, *β* = 100.004(2)°, *V* = 2876.3(6) $Å^3$, *Z* = 4, T = 213(2) K, θ_{max} = 28.27°, MoK*α* (λ = 0.71073 Å), 17252 measured reflections, 5059 independent reflections [R(int) = 0.0450], R_1= 0.0718, wR_2 = 0.1687, GOF = 1.172 ([$I > 2\sigma(I)$]). For **3a** (CCDC 675488): $C_{76}H_{60}ClN_2O_2P_2Rh_1S_2$, monoclinic, space group *C*2/c, *a* = 13.065(2) Å, *b* = 19.762(3) Å, *c* = 24.237(3) Å, *β* = 99.752(2)°, *V* = 6167.1(13) $Å^3$, *Z* = 4, T = 213(2) K, θ_{max} = 28.27°, MoK*α* (λ = 0.71073 Å), 23331 measured reflections, 7246 independent reflections [R(int) = 0.0505], R_1= 0.0585, wR_2 = 0.1254, GOF = 1.102 ([$I > 2\sigma(I)$]).

4.4. NMR experiment

4.4.1. ^{1}H NMR titration—Proton NMR titration was performed at 298 K. The condensed Rh(I) tweezer complex **3c** (5.15 mM) was titrated with *n*-$Bu_4N^+X^-$ (X = F, Cl, Br, and I) in CD_2Cl_2 by monitoring the changes in the chemical shift of amide −N*H* protons.

4.4.2. Job plot—Stock solution of **3c** (3.43 *m*M) and *n*-$Bu_4N^+Cl^-$ (3.44 *m*M) were prepared in CD_2Cl_2 solution separately. Eleven NMR samples ([**3c**]/([**3c**]+[*n*-$Bu_4N^+Cl^-$]) = 0.0, 0.1, 0.2, …, 0.9, 1.0) were prepared and ^{1}H NMR spectra were taken at room temperature.

4.5. Fluorescence measurement

4.5.1. Titration experiment—Stock solution of *n*-$Bu_4N^+X^-$(91.0 *m*M) and stock solution of **2**, **3d**, and **4d** (0.36 *m*M) were prepared in CH_2Cl_2 containing of 5% DMF. For all measurements, excitation was at 345 nm with excitation and emission slit width of 3 nm. Fluorescence titration experiments were performed with 5.4 *μ*M solutions of **2**, **3d** and **4d** and various concentrations of *n*-$Bu_4N^+X^-$ (X = F, Cl, Br, and I) in CH_2Cl_2 containing of 5% DMF.

Supplementary Material

Refer to Web version on PubMed Central for supplementary material.

Acknowledgments

C.A.M. acknowledges the ONR, NSF, and ARO for supporting this research and he is also grateful for a NIH Director's Pioneer Award. D.K. acknowledges the Korea Research Foundation Grant (KRF-2007-357-C00053) funded by the Korean Government (MOEHRD) for postdoctoral fellowship support.

References and notes

1. (a) Fujita M. Acc Chem Res. 1999; 32:53–61.(b) Pease AR, Jeppesen JO, Stoddart JF, Luo Y, Collier CP, Heath JR. Acc Chem Res. 2001; 34:433–444. [PubMed: 11412080] (c) Kesanli B, Lin WB. Coord Chem Rev. 2003; 246:305–326.(d) Lee JW, Samal S, Selvapalam N, Kim HJ, Kim K. Acc Chem Res. 2003; 36:621–630. [PubMed: 12924959] (e) Kovbasyuk L, Kramer R. Chem Rev. 2004; 104:3161–3187. [PubMed: 15186190] (f) Heath JR, Stoddart JF, Williams RS. Science. 2004; 303:1136–1137. [PubMed: 14976295] (g) Thanasekaran P, Liao RT, Liu YH, Rajendran T, Rajagopal S, Lu KL. Coord Chem Rev. 2005; 249:1085–1110.(h) Gianneschi NC, Nguyen ST,

Mirkin CA. J Am Chem Soc. 2005; 127:1644–1645. [PubMed: 15700991] (i) Amijs CHM, van Klink GPM, van Koten G. Dalton Trans. 2006:308–327. [PubMed: 16365645] (j) Heo J, Mirkin CA. Angew Chem, Int Ed. 2006; 45:941–944.(k) Oliveri CG, Gianneschi NC, Nguyen ST, Mirkin CA, Stern CL, Wawrzak Z, Pink M. J Am Chem Soc. 2006; 128:16286–16296. [PubMed: 17165783] (l) Filby MH, Steed JW. Coord Chem Rev. 2006; 250:3200.(m) Beer PD. Acc Chem Res. 1998; 31:71.(n) Gale PA, Garcia-Garrido SE, Garric J. Chem Soc Rev. 2008; 37:151. [PubMed: 18197339] (o) Wintergerst MP, Levitskaia TG, Moyer BA, Sessler JL, Delmau LH. J Am Chem Soc. 2008; 130:4129. [PubMed: 18311976]

2. (a) Holliday BJ, Mirkin CA. Angew Chem, Int Ed. 2001; 40:2022–2043.(b) Gianneschi NC, Masar MS, Mirkin CA. Acc Chem Res. 2005; 38:825–837. [PubMed: 16285706]
3. Masar MS, Gianneschi NC, Oliveri CG, Stern CL, Nguyen ST, Mirkin CA. J Am Chem Soc. 2007; 129:10149–10158. [PubMed: 17655295]
4. Yoon HJ, Heo J, Mirkin CA. J Am Chem Soc. 2007; 129:14182–14183. [PubMed: 17973396]
5. Holliday BJ, Farrell JR, Mirkin CA, Lam KC, Rheingold AL. J Am Chem Soc. 1999; 121:6316–6317.
6. (a) Farrell JR, Mirkin CA, Guzei IA, Liable-Sands LM, Rheingold AL. Angew Chem, Int Ed. 1998; 37:465–467.(b) Farrell JR, Mirkin CA, Liable-Sands LM, Rheingold AL. J Am Chem Soc. 1998; 120:11834–11835.(c) Jeon YM, Heo J, Brown AM, Mirkin CA. Organometallics. 2006; 25:2729–2732. [PubMed: 19060957] (d) Holliday BJ, Jeon YM, Mirkin CA, Stern CL, Incarvito CD, Zakharov LN, Sommer RD, Rheingold AL. Organometallics. 2002; 21:5713–5725.(e) Brown AM, Ovchinnikov MV, Mirkin CA. Angew Chem, Int Ed. 2005; 44:4207–4209.(f) Brown AM, Ovchinnikov MV, Stern CL, Mirkin CA. J Am Chem Soc. 2004; 126:14316–14317. [PubMed: 15521726] (g) Khoshbin MS, Ovchinnikov MV, Mirkin CA, Golen JA, Rheingold AL. Inorg Chem. 2006; 45:2603–2609. [PubMed: 16529482] (h) Khoshbin MS, Ovchinnikov MV, Mirkin CA, Zakharov LN, Rheingold AL. Inorg Chem. 2005; 44:496–501. [PubMed: 15679377] (i) Khoshbin MS, Ovchinnikov MV, Salaita KS, Mirkin CA, Stern CL, Zakharov LN, Rheingold AL. Chem-Asian J. 2006; 1:686–692. [PubMed: 17441109] (j) Ulmann PA, Brown AM, Ovchinnikov MV, Mirkin CA, DiPasquale AG, Rheingold AL. Chem-Eur J. 2007; 13:4529–4534. [PubMed: 17393545]
7. (a) Wegner SV, Okesli A, Chen P, He C. J Am Chem Soc. 2007; 129:3474–3475. [PubMed: 17335208] (b) Nagatoishi S, Nojima T, Juskowiak B, Takenaka S. Angew Chem, Int Ed. 2005; 44:5067–5070.(c) Kim SK, Lee SH, Lee JY, Lee JY, Bartsch RA, Kim JS. J Am Chem Soc. 2004; 126:16499–16506. [PubMed: 15600353]
8. Bader A, Lindner E. Coord Chem Rev. 1991; 108:27–110.
9. (a) Dixon FM, Eisenberg AH, Farrell JR, Mirkin CA, Liable-Sands LM, Rheingold AL. Inorg Chem. 2000; 39:3432–3433. [PubMed: 11196796] (b) Ovchinnikov MV, Brown AM, Liu XG, Mirkin CA, Zakharov LN, Rheingold AL. Inorg Chem. 2004; 43:8233–8235. [PubMed: 15606166]
10. (a) Szemes F, Hesek D, Chen Z, Dent SW, Drew MGB, Goulden AJ, Graydon AR, Grieve A, Mortimer RJ, Wear T, Weightman JS, Beer PD. Inorg Chem. 1996; 35:5868–5879.(b) Beer PD, Hesek D, Nam KC, Drew MGB. Organometallics. 1999; 18:3933–3943.(c) Mahoney JM, Beatty AM, Smith BD. Inorg Chem. 2004; 43:7617–7621. [PubMed: 15554626] (d) Suksai C, Leeladee P, Jainuknan D, Tuntulani T, Muangsin N, Chailapakul O, Kongsaeree P, Pakavatchai C. Tetrahedron Lett. 2005; 46:2765–2769.
11. Roesky HW, Andruh M. Coord Chem Rev. 2003; 236:91–119.
12. Hynes MJ. J Chem Soc Dalton Trans. 1993:311–312.b) The K_a of **3c** for Br^- and I^- are 2.69×10^3 M^{-2} and 2.03×10^3 M^{-2}, respectively.
13. Bisson AP, Lynch VM, Monahan MC, Anslyn EV. Angew Chem, Int Ed. 1997; 36:2340–2342.
14. Masar MS, Mirkin CA, Stern CL, Zakharov LN, Rheingold AL. Inorg Chem. 2004; 43:4693–4701. [PubMed: 15257598]
15. Doel CL, Gibson AM, Reid G. Polyhedron. 1995; 14:3139–3146.
16. (a) Del Zotto A, Nardin G, Rigo P. J Chem Soc, Dalton Trans. 1995:3343–3351.(b) Ruina Y, Kunhua L, Yimin H, Dongmei W, Douman J. Polyhedron. 1997; 16:4033–4038.
17. Errington, RJ. Advanced Practical Inorganic and Metalorganic Chemistry. Chapman & Hall; New York: 1997.

18. Armarego, WLF.; Perrin, DD. Purification of Laboratory Chemicals. Butterworth-Heinemann; Oxford: 1996.

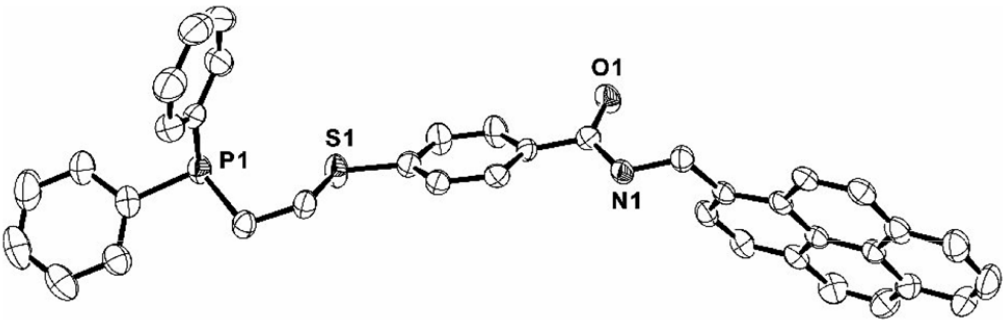

Figure 1.
ORTEP diagram for the crystal structure of **2**. Thermal ellipsoids are drawn at 60% probability. Hydrogen atoms have been omitted for clarity.

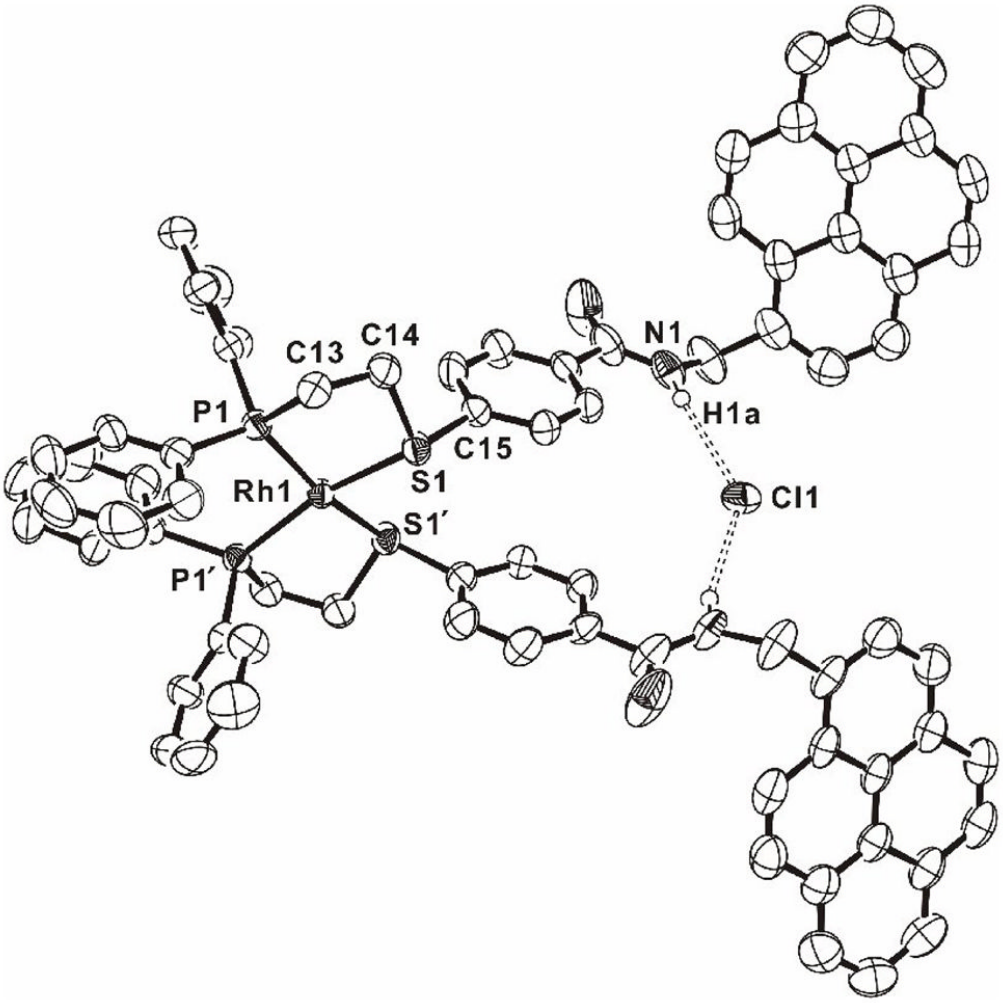

Figure 2.

ORTEP diagram for the crystal structure of **3a** with 60% probability ellipsoids. All but the amide hydrogen atoms have been omitted for clarity. Selected distances (Å) and angles (deg): Rh(1)-S(1) 2.330(5), Rh(1)-P(1) 2.232(3), Cl(1)…N(1) 3.241(4), P(1)-Rh(1)-S(1) 165.92(3), P(1)-Rh(1)-P(1′) 98.46(5), Rh(1)-S(1)-C(14) 105.70(11), Rh(1)-S(1)-C(15) 111.50(11), C(14)-S(1)-C(15) 102.07(17), Cl(1)-H(1a)-N(1) 162.40(4).

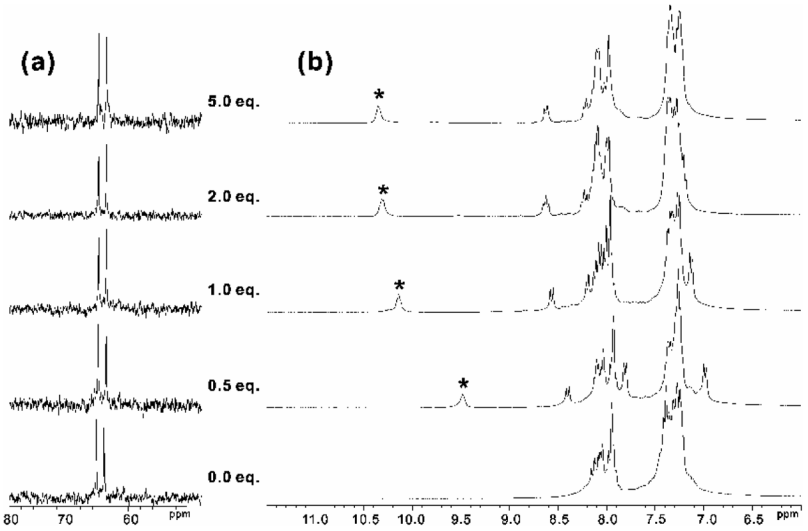

Figure 3.

Partial (a) $^{31}P\{^{1}H\}$ and (b) ^{1}H NMR spectra of **3c** (5.15 *m*M) in the presence of *n*-Bu_4NCl in CD_2Cl_2 at room temperature (The signals labeled with * represent the amide −N*H* protons).

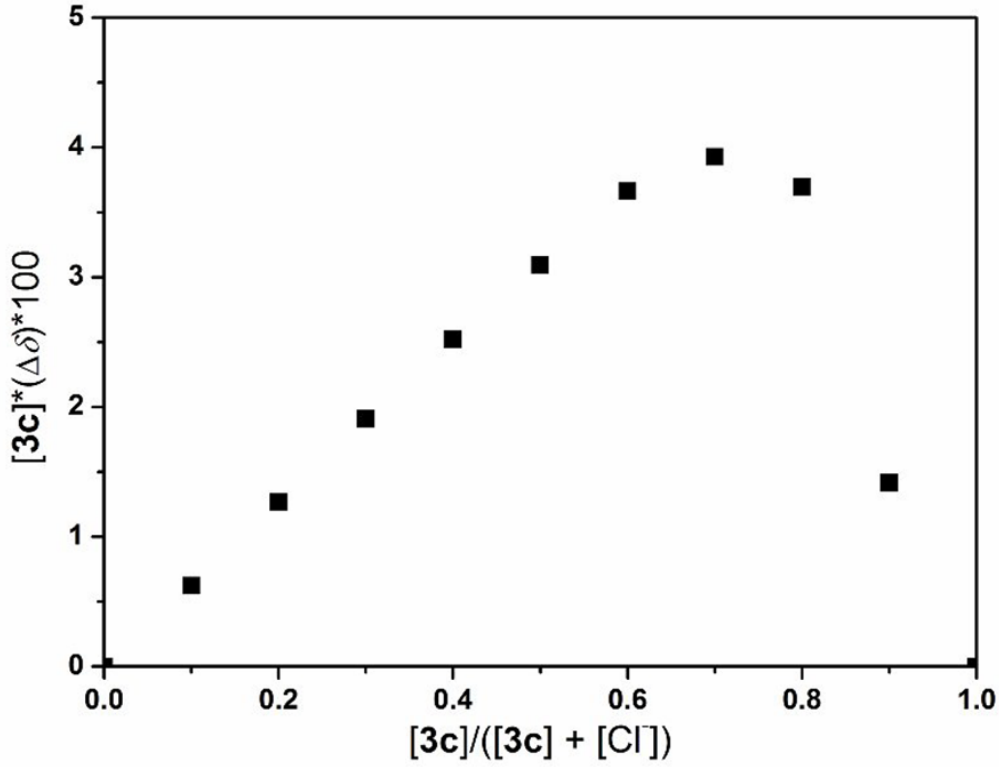

Figure 4.
Job plot for **3c** (3.43 *m*M) and *n*-Bu_4NCl (3.44 *m*M) in CD_2Cl_2 solution.

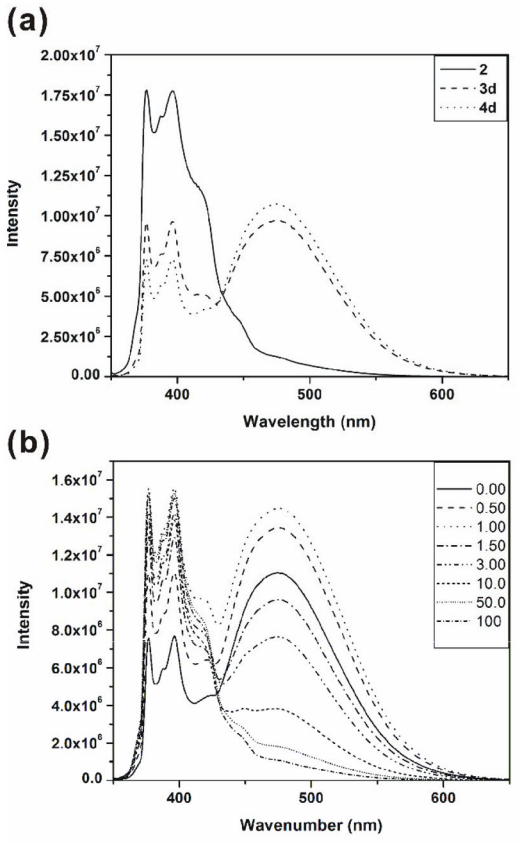

Figure 5.

(a) Fluorescence spectra of **2** (10.8 μM), **3d** (5.4 μM), and **4d** (5.4 μM). (b) Fluorescence spectral change of **4d** upon titration with *n*-Bu_4NCl in the CH_2Cl_2 containing of 5% DMF (excitation = 345 nm).

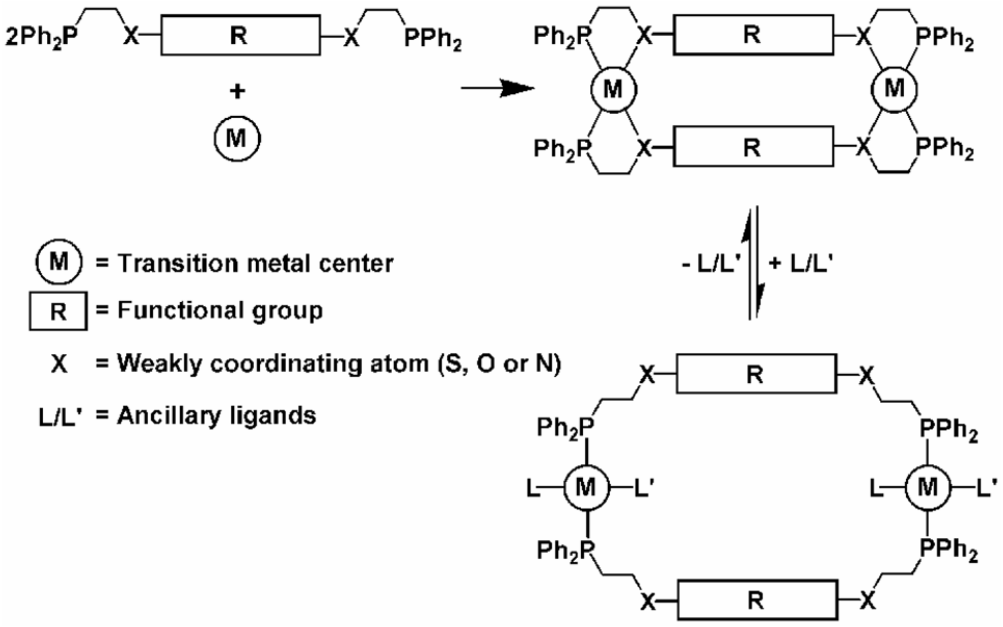

Scheme 1.
Schematic illustration of the Weak-Link Approach

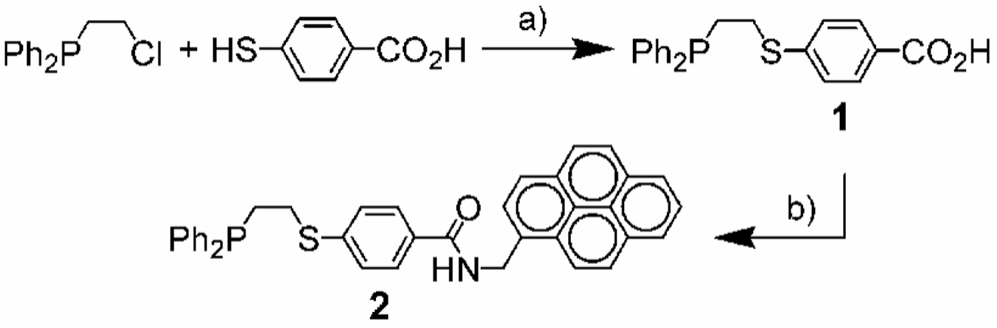

Scheme 2.
a) K_2CO_3, 18-Crown-6, CH_3CN/H_2O, reflux; b) Isobutylchloroformate/NEt_3, 2-Pyrenylmethylamine · HCl/NEt_3, CH_2Cl_2, rt.

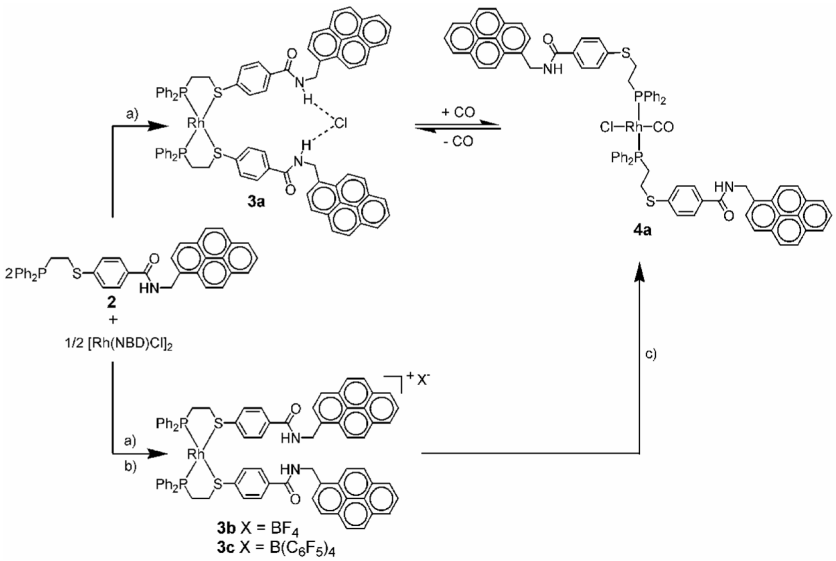

Scheme 3.

a) CH_2Cl_2, rt; b) $AgBF_4$ for **3b** and $LiB(C_6F_5)_4$ for **3c**; c) CO/*n*-Bu_4NCl, CH_2Cl_2, rt.

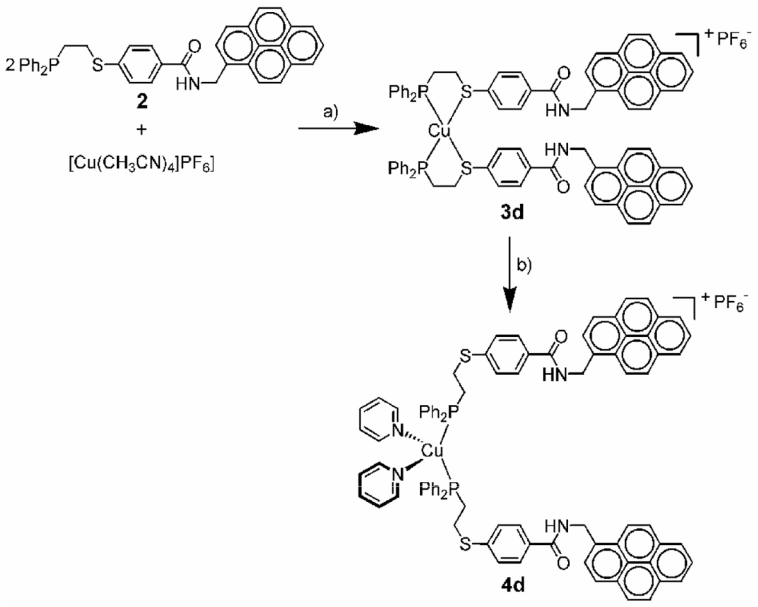

Scheme 4.
a) CH_2Cl_2, rt; b) Pyridine, CH_2Cl_2, rt.